This paper is part of the following report:

TITLE: Materials Research Society Symposium Proceedings. Volume 746. Magnetoelectronics and Magnetic Materials - Novel Phenomena and Advanced Characterization

To order the complete compilation report, use: ADA418228

The following component part numbers comprise the compilation report:
ADP014306 thru ADP014341

Mössbauer Characterization of Iron Oxide Nanoclusters Grown within Aluminosilicate Matrices

Georgia C. Papaefthymiou[1], A. Bustamante Dominguez[2] and Rosa B. Scorzelli[3]
[1]Department of Physics, Villanova University, Villanova, PA, USA.
[2]Facultad de Ciencias Fisicas, Universidad Mayor de San Marcos, Lima, Peru.
[3]Centro Brasileiro de Pesquisas Fisicas, Rio de Janeiro, Brasil.

ABSTRACT

Mössbauer spectroscopy uses the resonant absorption of nuclear radiation by ^{57}Fe to probe the electronic and internal magnetic structure of iron based magnetic materials. The technique has a characteristic measuring time of 10 ns enabling investigation of spin relaxation phenomena in nanoscale particles; and determination of their magnetic properties in the absence of externally applied magnetic fields. We report on Mössbauer studies of γ-Fe_2O_3 nanoparticles synthesized within hexagonally packed mesoporous MCM-41 aluminosilicate matrices with cylindrical pores of 2.5 nm diameter. Data analysis allowed differentiation of particle-matrix interfacial versus particle-core interior iron sites. Interfacial iron atoms experience large electric field gradients resulting in quadrupole splitting values of ΔE_q (surface) = (1.25 $\pm$ 0.05) mm/s, while core atoms exhibit smaller values of ΔE_q (core) = (0.73 $\pm$ 0.05) mm/s at room temperature. Similarly, differences were observed in the values of the internal hyperfine fields at low temperatures indicating reduced strength in the exchange interactions at the particle surface, with interfacial atoms experiencing internal fields H_{hf} (surface) = (458 $\pm$ 1) kOe reduced relative to the core H_{hf} (core) = (488 $\pm$ 1) kOe at 4.2 K. Particle/matrix interactions at the surface appear to perturb the electronic interactions deeper into the core than the magnetic exchange interactions.

INTRODUCTION

Porous matrices are ideal hosts for the dispersion of nanoclusters. Zeolitic and sol-gel derived molecular sieves and a variety of cross-linked and block co-polymers have been used to this purpose [1-4]. The matrices vary from micro- to meso-porous and from amorphous to highly ordered, affording nanocomposites with a wide range of physical properties. Nanotechnological applications, ranging from catalysis to novel electronic devices and magnetic media, drive the exploration of these advanced materials [5]. We have made use of hexagonally packed MCM-41 aluminosilicate matrices [6] for the production of well-organized nanocluster assemblies of Fe_2O_3. By packing the nanoclusters within the host matrix the interfacial confinement environment is expected to lead to uniquely tailored morphology and magnetic behavior. In particular, the 1D-cylindrical pore channels of the hexagonally packed aluminosilicate matrices could afford the encapsulation of extremely elongated nanoparticles, leading to the production of magnetic nanorods or nanowires, as one of us and collaborators have previously reported [1]. Herewith, we present fundamental studies on the electronic and magnetic properties of the $Fe_2O_3/AlSiO_2$ nanocomposites based on Mössbauer spectroscopic measurements. Specifically, we address the characterization of the particle/matrix interfacial region and present a more thorough interpretation of Mössbauer results presented in [1]. Particle/matrix interactions impose large stress on the surface perturbing the electronic and magnetic interactions over a

finite shell of atomic lattice planes; they also appear to perturb the electronic interactions over a longer range from the particle surface than the magnetic exchange interactions.

MATERIALS AND METHODS

Mesoporous silica 25% doped with Al (AlSi-25) was synthesized from an inorganic siliceous precursor using organic cationic trimethylammonium surfactants as a supermolecular templating agent. Details of the synthesis and characterization of the resulting MCM-41 aluminosilicate matrix have been presented elsewhere [1]. The matrix had a narrow pore size distribution centered at about 2.5 nm pore diameter for the 1D-channels. Introduction of iron oxide within the pore structure of the matrix was achieved via evaporation/condensation of volatile $Fe(CO)_5$. TEM bright field images of as prepared and 500 °C calcined Fe_2O_3/AlSi-25 nanocomposites indicated the presence of a hexagonally packed array with dark phase contrast inside the pores, corresponding to the iron oxide guest structure (Fig. 1). No particle agglomeration or sintering was observed after calcination in a tube oven under flowing oxygen for 3 hours at 500 °C. X-ray probe iron mapping and STEM images perpendicular to the hexagonally packed arrays (see reference [1]) indicated the presence of both spherical and elongated morphologies for the iron oxide particles.

We have used Mössbauer spectroscopy in order to examine the electronic and magnetic properties of the Fe_2O_3/AlSi-25 nanocomposites. Mössbauer spectroscopy [7] uses the resonant absorption of nuclear radiation by the ^{57}Fe-nucleus to probe the electronic and internal magnetic structure of iron based magnetic materials. This is accomplished by the determination of the electronic and magnetic hyperfine parameters at the iron site: isomer shift, δ, quadrupole splitting, ΔE_q, and hyperfine field, H_{hf}. Correlated values of all three Mössbauer parameters can be used for structural phase determination. This is particularly valuable in the study of nanostructures, as crystallites of nanometer size dimensions are not amenable to XRD structural determination, due to line broadening produced by the small particle diameter.

Mössbauer spectroscopy has a fast characteristic measurement time, $\tau_{Möss} = 10$ ns, which enables examination of dynamic and static magnetic properties of nanostructures over a convenient temperature range. This may be compared to routine macroscopic magnetization studies using Superconducting Quantum Interference Device (SQUID) magnetometers which have longer measurement times, $\tau_{Mag} = 10$ s to 100 s. Thus, Mössbauer blocking temperatures of

Figure 1. TEM micrographs of Fe_2O_3/AlSi-25 nanocomposites: (left) as prepared and (right) calcined at 500 °C.

magnetic nanostructures would be higher than those for SQUID measurements. Another important feature of the technique is that magnetic characterization is achieved in the absence of an externally applied field, obviating the need for zero-field extrapolation of the data.

Due to their extremely small size, nanometer size particles have a large fraction of surface to interior iron atoms. We have assumed a simple idealized core-shell model according to which the core is highly crystalline and uniformly magnetized, while the shell is somewhat amorphous with surface atom coordination severely distorted leading to large ligand-field splittings and iron spins strongly pinned at the surface [8]. Such surface atom coordination distortions would be reflected in ΔE_q and H_{hf} values for atoms at the particle-matrix interface versus those in the interior of the particle [9]. Mössbauer spectra were recorded for 4.2 K< T < 300 K using a continuous flow liquid helium cryostat. The experimental data were computer fitted to theoretical spectra using a non-linear, least-squares curve fitting procedure.

RESULTS AND DISCUSSION

Fitted Mössbauer spectra for the as-prepared sample are shown in Figure 2. The overall temperature profile is characteristic of magnetically ordered iron oxide particles [10] undergoing superparamagnetic relaxation processes due to thermally driven particle moment reversals [11]. The superparamagnetic relaxation time is given by $\tau_s = \tau_0 \exp (KV/kT)$, where T is the temperature, V the volume and K the magnetic anisotropy density of the particle; k is Boltzmann's constant and τ_0 is a temperature independent constant characteristic of the material.
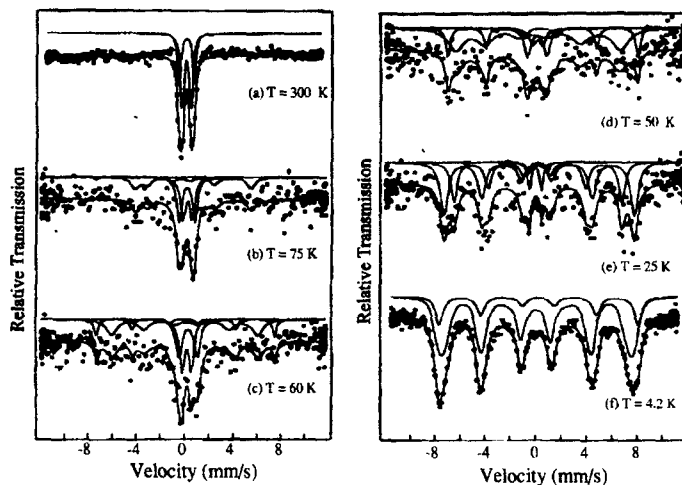

Figure 2. Mössbauer spectra of as-prepared Fe_2O_3/AlSi-25 nanocomposites. The solid line is a least-square fit to the experimental points, assuming a superposition of sites depicted by the theoretical spectra shown above the experimental data. The magnetic subcomponents were fitted to a distribution of magnetic hyperfine fields in order to simulate intermediate relaxation effects.

At low temperatures particle-moment reversals are slowed down revealing the internal magnetic order of the particle when $\tau_s > 10$ ns.

At room temperature, broad quadrupole doublets were obtained. The large absorption line-width necessitated fitting to the superposition of two unresolved doublets of similar isomer shift, but different quadrupole splittings (TABLE I). The values of ΔE_q's reflect the degree of iron coordination distortion away from perfect octahedral or tetrahedral coordination. Thus, larger ΔE_q values were associated with the surface (shell) atoms; smaller ones with interior (core) atoms. The relative absorption intensity of shell vs. core atoms, determined by the ratio of the areas of absorption under the associated curves, gives the relative population of surface to core iron atoms within the assumption of similar recoil free-fractions [7]. Spectral fits at room temperature give A (shell) : A (core) = 40 : 60.

The six line magnetic spectra at low temperatures were also fit within the core-shell model to the superposition of two magnetic subsites with two internal hyperfine magnetic fields associated with core and shell iron atoms, respectively (TABLE I). The sharp discontinuity in the Fe-O-Fe superexchange paths of the magnetic lattice at the surface of the particle leads to a canted surface-spin structure with diminished strength of the magnetic exchange interactions at the surface. The contribution from surface atoms to the magnetic absorption spectral area was suppressed compared to that observed for the paramagnetic spectra at room temperature, resulting in A (shell) : A (core) = 20 : 80 at 4.2 K.

We have previously interpreted this reduction of surface to core ratio [1] as an indication of the presence of a frozen core spin-structure; while, surface spin fluctuations [12] still persisted at 4.2 K. That is, even though spins at the surface are canted relative to the magnetic easy axis of the core due to pinning forces at the surface, the lower magnetic fields observed at the surface could result in spin fluctuations about local easy axes being thermally accessible at lower temperatures than within the core where the observed internal hyperfine fields are 6% stronger. This, however, appears to be in contradiction to strong pinning at the surface. An alternative, and probably most likely interpretation, is that the discontinuity at the surface disturbs the

TABLE I. Mössbauer Parameters for Fe_2O_3/AlSi-25 Nanocomposite

Fe_2O_3/AlSi-25 Nanocomposite	T (K)	Isomer Shift [a,b] δ (mm/sec)		Quadrupole Splitting [a] ΔE_q (mm/sec)		Hyperfine Field [a] H_{hf} (kOe)	
		Surface	Core	Surface	Core	Surface	Core
As-prepared	300	0.33	0.33	1.25	0.73	---	---
	4.2	(0.45)	(0.45)	0	-0.026	458	488
Calcination at 300 °C	300	0.36	0.34	1.24	0.74	---	---
	4.2	(0.48)	(0.46)	0	-0.056	448	477
Calcination at 500 °C	300	0.39	0.35	1.10	0.81	---	---
	4.2	(0.51)	(0.47)	0	-0.132	442	488
Bulk γ-Fe_2O_3 (A+B sites averaged)	298	0.35[c]		0		496[d]	

[a] Uncertainties in δ, ΔE_q and H_{hf} are ± 0.03 mm/sec , ± 0.05 mm/sec and ± 1.0 kOe, respectively.
[b] Isomer shift is relative to metallic iron at room temperature; 4.2 K values were fixed at those obtained at room temperature + 0.12 mm/sec second-order Doppler shift. [c] Reference [13]. [d] Reference [14].

electric field gradients deeper into the core than the strength of the magnetic exchange interactions. Thus, the thickness of the shell derived from the quadrupolar spectra would appear larger than that derived from analysis of the magnetic spectra.

At intermediate temperatures, the spectra are more complex due to intermediate spin relaxation phenomena and the presence of a distribution of particle sizes. The relaxation profiles have been fitted to superpositions of paramagnetic and magnetic subcomponents. Intermediate relaxation processes have been simulated phenomenologically by introducing a distribution of hyperfine field values. The outer absorption magnetic field lines in Fig. 2 are observed to shift inward with increasing temperature, indicating that the average hyperfine fields decrease with increasing temperature. This is an indication that at low temperatures, where spin reversals are suppressed, the particle magnetization may still undergo collective magnetic excitations about its easy axis of magnetization [13].

The Mössbauer parameters of the as-prepared nanocomposite are consistent with maghemite (γ-Fe$_2$O$_3$). This phase identification is supported by: (i) the absence (or negligible) quadrupolar perturbation on the magnetic spectra and (ii) the values of the hyperfine fields observed. Hematite (α-Fe$_2$O$_3$) exhibits a large quadrupolar perturbation of 0.12 mm/sec at 300 K and -0.22 mm/sec below the Morin transition [7]; and a saturation hyperfine field H_{sat}=544 kOe. In contrast, γ-Fe$_2$O$_3$ has zero quadrupolar perturbation and H_{sat} = 527 kOe. Furthermore, it is well known that α-Fe$_2$O$_3$ is a canted antiferromagnet exhibiting weak bulk magnetization, while the present sample recorded a magnetization value of 57emu/g at 4.2 K in SQUID measurements (see reference [1]) consistent with ferrimagnetic γ-Fe$_2$O$_3$.

Furthermore, the phase of the iron oxide appeared to be stable at higher temperatures in transmission electron microscope and Mössbauer studies. Mössbauer parameters obtained for samples calcined for 3 hours in flowing oxygen at 300 and 500 °C are given in Table I. The small changes in parameter values observed appear to be consistent with increased particle crystallinity, due to atomic restructuring upon calcination at high temperatures.

CONCLUSION

Mössbauer spectroscopy affords structural, electronic and micromagnetic characterization of iron based, artificially structured magnetic materials. Spectral fitting procedures within a core/shell model hypothesis for this γ-Fe$_2$O$_3$/AlSi-25 nanocomposite allowed electronic and magnetic characterization of the embedded particle/matrix interfaces. Quadrupole splitting values at the surface increased by 37%, while magnetic field values decreased by 6%, relative to the interior; pointing to severe iron-ion coordination distortion at the surface and large surface stress or strain imposed by the supporting matrix. The core/shell model analysis yielded estimates of the fraction of atoms lying on the surface. Based on electronic measurements 40% of atoms lie on the surface, while internal magnetic field measurements yield a smaller number of only 20%. This is consistent with the hypothesis that the strength of the magnetic exchange interactions are modified to a lesser degree and over a shorter distance from the surface into the core as compared to the electronic interactions.

The observed distortions at the surface are consistent with the existence of large strains at the surface known to result in strong surface contributions to the magnetic anisotropy densities in small magnetic particles as compared to the bulk [15]. Even spherical particles of nanometer dimensions, lacking shape anisotropy, exhibit magnetic anisotropy constants two orders of magnitude larger than the corresponding bulk material [10]. Large distortions of the crystalline

lattice at the surface of the particle, as observed in this nanocomposite, originating from particle/matrix interfacial interactions could account for such effects. The same interactions and geometrical confinement of the particles within the aluminosilicate matrix could account for the increased stability of the particles at high temperatures.

ACKNOWLEDGEMENTS

REFERENCES

1. L. Zhang, G. C. Papaefthymiou and J. Y. Ying, *J. Phys. Chem. B.*, **105**, 7414 (2001) and references there in.
2. L. Zhang, G. C. Papaefthymiou and J. Y. Ying, *J. Appl. Phys.*, **81**, 6892 (1997); L. Zhang, G. C. Papaefthymiou, R.F. Ziolo and J. Y. Ying, *Nanostr. Mater.* **9**, 185 (1997).
3. B. H. Sohn, R. E. Cohen and G. C. Papaefthymiou, *J. Mag. Mag. Mat.*, **182**, 216 (1998) and references there in.
4. S.R. Ahmed, S.B. Ogal, G.C. Papaefthymiou, R. Ramesh and P.Kofinas, *Appl. Phys. Lett.*, **80**, 1616 (2002)
5. G. C. Hadjipanayis, R. W. Siegel; Eds. *Nanophase Materials: Synthesis-Properties-Applications*; Kluwer: Boston, 1994; H. Gleiter, *Mater. Sci. Forum*, **67**, 189 (1995); C. L. Chien, *Ann. Rev. Mater. Sci.*, **129**, 25 (1995); D. L. Leslie-Pelecky and R.D. Rieke, *Chem. Mater.*, **8**, 1770 (1996); A.S. Edelstein R.C. Camarata, Eds. *Nanomaterials: Synthesis, Properties and Applications*. Institute of Physics Publishing: Bristol (1996)
6. C. T. Kresge, M. E. Leonowicz, W. J. Roth, J. C. Vartuli and J. S. Beck, *Nature*, **359**, 710 (1992).
7. N. N. Greenwood and T. C. Gibb, *Mössbauer Spectroscopy*; Chapman Hall: London, 1971.
8. J. M. D. Coey, *Phys. Rev. Lett.*, **27**, 1140 (1971).
9. G. C. Papaefthymiou, *Mat. Res. Soc. Symp. Proc.* **635** (2001) C2.4.1
10. J. L. Dormann and D. Fiorani; Eds. *Magnetic Properties of Fine Particles*; Elsevier: North-Holland, 1992.
11. L. Néel, *Ann. Geophys.* (France) **5**, 99 (1949); I.S. Jacobs and C.P. Bean, in *Magnetism III*, edited by G.T. Rado and H. Suhl (Academic Press, New York, 1963) p. 271; W.F. Brown Jr. *Phys. Rev.* **130**, 8061 (1963); A. Aharoni, *Phys. Rev.* A **135**, 447 (1964)
12. L.J. de Jongh and A.R. Miedema, *Adv. Phys.*, **1**, 23 (1974).
13. S. Mørup and H. Topsøe, *J. Appl. Phys.*, **11**, 63 (1976).
14. H. V. Kelly, V. J. Folen, M. Hass, W. N. Schreiner and G. B. Beard, *Phys. Rev.*, **122**, 1447 (1961).
15. E.C. Stoner, F.R.S. and E.P Wohlfarth, *Phil. Trans. Roy. Soc. London*, **A240**, 599 (1948); reprinted in *IEEE Trans. Magn.*, **27**, 3475 (1991)